MODELING OF SPARK GAP PERFORMANCE*

A. L. Donaldson, R. Ness, M. Hagler, M. Kristiansen
Department of Electrical Engineering

and

L. L. Hatfield
Department of Physics
Texas Tech University
Lubbock, Texas 79409

Abstract

A model which incorporates the influence of electrode surface conditions, gas pressure, and charging rate on the voltage stability of high energy spark gaps is discussed. Implications of the model include changes in the width of the self-breakdown voltage probability density function as the secondary emission characteristics of the cathode are modified by, for example, oxide and nitride coatings and/or deposits from the insulator. The model indicates that a narrow self-breakdown voltage distribution requires a source of electrons near the cathode surface, which could be provided by UV photo-illumination of the cathode. In addition, the model provides an extremely useful, and physically reasonable framework, from which the properties of spark gaps under a wide variety of experimental conditions may be evaluated. Both experimental and theoretical results are presented.

Introduction

Low-jitter, triggered spark gaps are needed for a wide variety of switching applications including fusion machines [1], weapons systems, and high energy physics experiments. To achieve low jitter, the switch should be triggered as close to the self-breakdown voltage as possible; thus, an ideal switch should have a delta function for the self-breakdown voltage probability density function. In actual operation the self-breakdown voltage will be somewhat erratic and in most cases "prefires", or breakdown voltages which are significantly less than the mean, will occur. The self-breakdown voltage density functions and the respective distributions for these cases are shown in Figure 1.

Numerous studies [2-5] have shown that the choice of gas, electrode and insulator material can significantly influence the width and shape of the actual voltage density function. More specifically, several studies [6-8] have suggested a correlation of the statistical distribution in the self breakdown voltage of a spark gap and the properties of the cathode surface, including its microstructure. The data have been interpreted in terms of models that consider:

1) the effect of the cathode surface properties on the primary election emission current, i_e, at the cathode [6,9,10], and
2) the effects of the field enhancement due to cathode surface microstructure on Townsend's first ionization coefficient, [6,11,12].

Both models include the concept of waiting-for-an-electron, in that breakdown is assumed to occur when the first electron appears at the cathode after a breakdown condition (usually the Townsend condition)

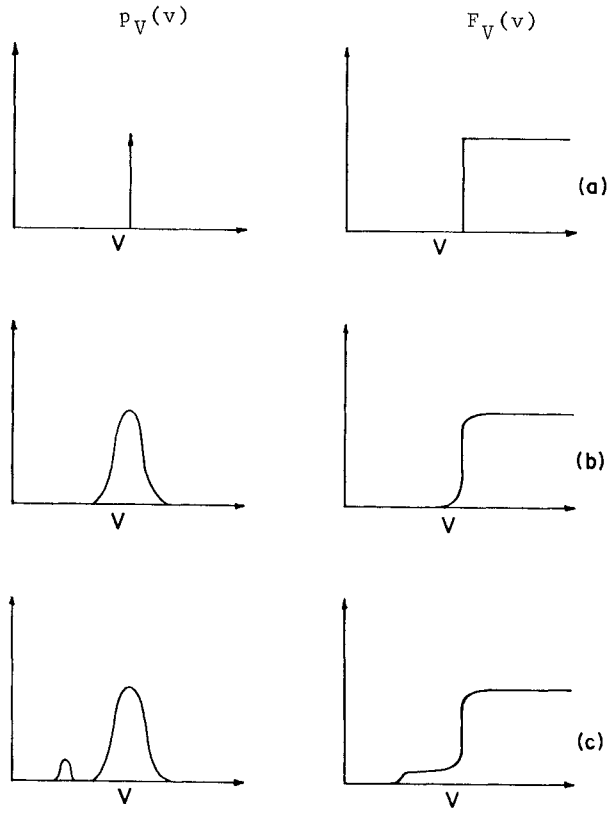

Fig. 1. The Self-Breakdown Voltage Probability Density Function, $p_V(v)$, and its Distribution Function, $F_V(v)$ for a) Ideal Spark Gap, b) Actual Spark Gap, c) Actual Spark Gap with Prefires.

has been satisfied. The theoretical model and the experimental results presented here includes both of these mechanisms by which the cathode surface can affect the statistical distribution in the breakdown voltage and, in addition, includes the field enhancement effects on the cathode surface in a new way.

Theoretical Model

General Case

Consider a spark gap subjected to a monotonically increasing applied voltage, v(t). Denote the breakdown voltage, a random variable, as V. The field enhancement factor, M, on the cathode surface is also considered to be a random variable. (The underlying sample space is the geometrical surface of the cathode.) The random variable M is characterized by a probability density function, $p_M(m)$. A basic assumption of the model is that the gap breaks down when an electron is born at a site on the cathode surface where M is as large as or larger than the value that satisfies the breakdown condition (Townsend

*Supported by: The Air Force Office of Scientific Research

Report Documentation Page

Form Approved
OMB No. 0704-0188

1. REPORT DATE	2. REPORT TYPE	3. DATES COVERED
JUN 1983	**N/A**	**-**

4. TITLE AND SUBTITLE	5a. CONTRACT NUMBER
Modeling Of Spark Gap Performance	5b. GRANT NUMBER
	5c. PROGRAM ELEMENT NUMBER
6. AUTHOR(S)	5d. PROJECT NUMBER
	5e. TASK NUMBER
	5f. WORK UNIT NUMBER
7. PERFORMING ORGANIZATION NAME(S) AND ADDRESS(ES) **Department of Electrical Engineering Texas Tech University Lubbock, Texas 79409**	8. PERFORMING ORGANIZATION REPORT NUMBER
9. SPONSORING/MONITORING AGENCY NAME(S) AND ADDRESS(ES)	10. SPONSOR/MONITOR'S ACRONYM(S)
	11. SPONSOR/MONITOR'S REPORT NUMBER(S)

12. DISTRIBUTION/AVAILABILITY STATEMENT
Approved for public release, distribution unlimited

13. SUPPLEMENTARY NOTES
See also ADM002371. 2013 IEEE Pulsed Power Conference, Digest of Technical Papers 1976-2013, and Abstracts of the 2013 IEEE International Conference on Plasma Science. Held in San Francisco, CA on 16-21 June 2013. U.S. Government or Federal Purpose Rights License

14. ABSTRACT
A model which incorporates the influence of electrode surface conditions, gas pressure, and chaJ:ging rate on the voltage stability of high energy spark gaps is discussed. Implications of the model include changes in the width of the self-breakdown voltage probability density function as the secondary emission characteristics of the cathode are modified by, for example, oxide and nitride coatings and/or deposits from the insulator. The model indicates that a narrow self-breakdown voltage distribution requires a source of electrons near the cathode surface, which could be provided by UV photo-illumination of the cathode. In addition, the model provides an extremely useful, and physically reasonable framework, from which the properties of spark gaps under a wide variety of experimental conditions may be evaluated. Both experimental and theoretical results are presented.

15. SUBJECT TERMS

16. SECURITY CLASSIFICATION OF:			17. LIMITATION OF ABSTRACT	18. NUMBER OF PAGES	19a. NAME OF RESPONSIBLE PERSON
a. REPORT	b. ABSTRACT	c. THIS PAGE			
unclassified	**unclassified**	**unclassified**	**SAR**	**5**	

perhaps) at the particular voltage applied. We denote this threshold value of the field enhancement as $m_t(v)$. Physically we expect that $m_t(v)$ is a monotonically decreasing function of v ($\partial m_t(v)/\partial v<0$), an increasing function of pressure ($\partial m_t(v)/\partial p>0$), and that $m_t(0)=\infty$ and $m_t(\infty)=0$. The actual calculation of $m_t(v)$ has been derived and explained elsewhere [8,13].

We now calculate the probability, p_t, that the gap breaks down during the time between t and t + Δt and hence at a voltage between v and v + Δv. For Δt small, the probability that an electron is born between t and t + Δt at a site where M takes a value between m and m + Δm is

$$\frac{i_e(m,v(t))}{e}\,\Delta t\; p_M(m)\Delta m \qquad (1)$$

The quantity e is the charge on an electron and i_e, the primary electron current generated at the cathode, is allowed to depend on both the field enhancement, M, at the cathode surface and on the applied voltage, v(t). Thus, the probability that the gap breaks down between t and t + Δt is

$$p_t(\Delta t) = \frac{\Delta t}{e}\int_{m_t(v)}^{\infty} i_e(m,v(t))p_M(m)dm \qquad (2)$$

It can be shown [13] that this leads to the expression for the voltage density function $p_V(v)$:

$$p_V(v) = \frac{\lambda(v)}{v'}\exp\left[-\int_0^v \frac{\lambda(\eta)d\eta}{v'}\right] \qquad (3)$$

where

$$\lambda(v) = \frac{1}{e}\int_{m_t(v)}^{\infty} i_e(m,v)p_M(m)dm \qquad (4)$$

It is easy to see that

$$F_V(v) = \int_0^v p_V(\xi)d\xi = 1 - \exp\left[-\int_0^v \frac{\lambda(\eta)d\eta}{v'(\eta)}\right] \qquad (5)$$

where $F_V(v)$ is the cumulative probability distribution for the random variable, V. Note that v'is to be evaluated at v, and hence can be considered as a function of v(v'=v'(v)).

If v(t) is a ramp, then v'=v_0', a constant. If v(t) is an RC charging waveform, then v'=(v_0-v)/RC where v_0 is the charging voltage.

These equations for $p_V(v)$ and $F_V(v)$ represent the model's prediction of the voltage self-breakdown statistics for the gap in terms of the primary electron current, $i_e(m,v)$; the probability density function $p_M(m)$ of the cathode field enhancement, considered as a random variable; the threshold field enhancement, $m_t(v)$, expressed as a function of the voltage applied in the gap; and the time derivative, v', of the applied voltage. From these equations it is easy to show that

$$\frac{1}{e}\int_{m_t(v)}^{\infty} i_e(m,v)p_M(m)dm = \frac{v'p_V(v)}{1-F_V(v)} \qquad (6)$$

Notice that the right hand side of Eq. (6) can be measured experimentally.

Special Cases

To proceed further, consider two special cases of the model. First, suppose that $i_e(m,v)$ is constant so that field enhancement distribution effects from the cathode surface microstructure and waiting-for-an-electron effects are the primary physical mechanisms included in the model. This circumstance is likely to hold, for example, when the cathode is illuminated with sufficiently intense ultraviolet radiation so that any field emission current is dwarfed by photoelectric current, which should be independent of M and v. If $i_e = i_{eo}$, a constant, then Eq. (6) gives

$$F_M(m_t(v)) = 1 - \frac{e}{i_{eo}}\frac{v'p_V(v)}{1-F_V(v)} \qquad (7)$$

where $F_M(m)$ is the cummulative probability distribution for the random variable, M. If we know $m_t(v)$, we can determine $F_M(m)$ by plotting $F_M(m_t(v))$ vs $m_t(v)$. For this special case, therefore, it is possible, in principle, to deduce $F_M(m)$ from $p_V(v)$ (self breakdown voltage histogram) under a given set of conditions and thus predict $p_V(v)$ (or $F_V(v)$) for a different v' or gas pressure (which affects $m_t(v)$), for example. For this special case, Eq. (5) becomes

$$F_V(v) = 1-\exp\left[-\frac{i_{eo}}{e}\int_0^v \frac{[1-F_M(m_t(\eta))]d\eta}{v'}\right] \qquad (8)$$

Consider now a second special case in which $p_M(m) = \delta(m - m_0)$, where $\delta(\cdot)$ is the Dirac delta function and m_0 is a constant. In this case the field enhancement is assumed to be uniform (that is, sufficiently characterized by its mean value rather than its distribution) so that the primary effects included are the voltage dependence of the primary electron current, i_e, and waiting-for-an-electron. In this case Eq. (5) becomes

$$F_V(v) = 1-\exp\left[-\frac{1}{e}\int_{v_t}^v \frac{i_e(m_0,\eta)d\eta}{v'}\right] \qquad (9)$$

where v_t is the threshold voltage, and $m_t(v_t)=m_0$, while Eq. (6) becomes

$$i_e(m_0,v) = \frac{ev'p_V(v)}{1-F_V(v)} \qquad (10)$$

Experimental Arrangement

The experimental arrangement and the system diagnostics used to test the theoretical results are shown in Figures 2 and 3. The construction of this facility and the development of the modeling software is described elsewhere [8,14]. The test circuit shown in Figure 3 consists of a high energy (2kJ) pulse forming network (PFN) and a low energy (<1mJ) RC probing circuit. The PFN is used to generate an electrode surface which is characteristic of a high energy switch. The RC probing circuit is used to generate the voltage distributions with a low energy, low current pulse so that the steady state temperature is reached prior to each shot. This low energy circuit is also used so that the surface microstructure will not be altered significantly from shot to shot. The pressure in the spark gap could be raised to 3.5 atmospheres and the voltage ramp rate could be varied from 3 to 60 kV/sec by changing R_c. A 5 Watt UV lamp was used to generate additional electrons at the cathode surface when needed.

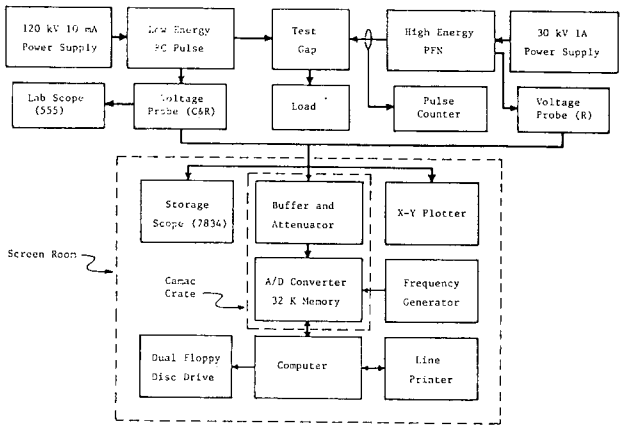

Fig. 2. Experimental Arrangement and System Diagnostics.

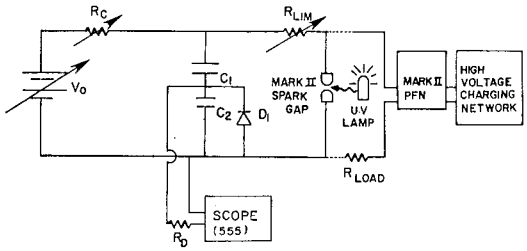

Fig. 3. Test Circuits.

A testing sequence consisted of firing 2000-7000 shots at high energy, waiting for approximately 1 hour for the electrode to cool, and proceeding with several series of 500, low energy shots with different i_e, v' and pressure. A typical electrode surface generated by the high energy pulses for the case of 304 stainless steel run in 1 atmosphere of nitrogen gas at a gap separation of 5mm is shown in Figure 4. Examination of the electrode surface after application of the low energy pulses indicates that no significant changes had occurred which might alter the breakdown statistics.

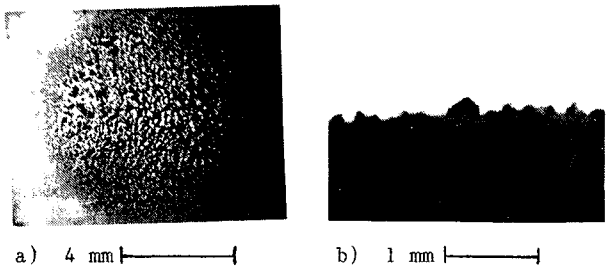

Fig. 4. Stainless Steel Electrode Run in Nitrogen, a) Cathode Surface-Top View, b) Cathode Surface-Side View.

Experimental Results

Several experiments were performed to verify the model's predictions for the effect of i_e, v', and pressure on the probability density function $p_V(v)$. In the first experiment, an UV source was used to generate a continuous supply of photoelectrons at the surface of a stainless steel electrode in air. Figure 5 shows that without UV, the density function is very broad indicating that the cathode surface is a very poor emitter of electrons. However, with the UV source on, the density function collapsed to the lowest value of breakdown voltage. This result is significant for at least two reasons. First, it supports the waiting-for-an-electron concept as one mechanism responsible for statistical variation in the self-breakdown voltage, and second, it provides an externally controllable experimental "switch" where the effect of waiting-for-an-electron can be turned on or off. The behavior observed is consistent with Eq. (5).

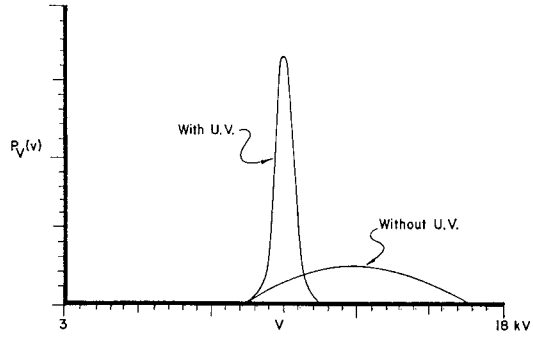

Fig. 5. Self Breakdown Voltage Probability Density Function For Stainless Steel in Air With and Without UV.

A second experiment consisted of varying the voltage ramp rate v' from 3 kV/sec ("slow" ramp) to 30 kV/sec ("fast" ramp). According to the model (Eq. (5)), if you are waiting for an electron to appear, then the faster the ramp rate, the higher the breakdown voltage will be when the electron appears and thus the greater the scatter in the density function $p_V(v)$. Figure 6 shows that this effect was indeed observed. Also, from Eq. (5) the density function for the slower ramp rate could be theoretically calculated from the data for the fast ramp rate. Figure 6 shows this result for the assumption $i_e = i_{eo}$, a constant. The result is fair at best which indicates that for better agreement a more realistic expression for i_e, perhaps $i_e(m,v)$, would have to be used.

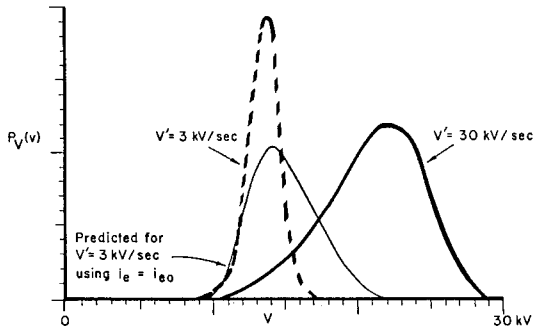

Fig. 6. Self Breakdown Voltage Probability Density Function For Different Charging Rates.

Previous work [12,15-17] has shown that with the presence of cathode microstructure, an increase in pressure can lead to significant deviations from the Paschen curve breakdown voltage if the product of the protrusion height and the pressure is greater than a gas dependent threshold. Avrutskii (7) stated that an increase in pressure should lead to an increase in scatter in the breakdown voltage but no data were given. Thus, in order to understand the effect of pressure on the breakdown voltage statistics for a surface with large protrusions, a brass sample was generated and the breakdown voltages were recorded for pressures up to 3.5 atmospheres. (Earlier work in electrode erosion had shown that brass electrodes in high energy operation could form protrusions up to

500 μm (14).) Figure 7 clearly shows an increase in scatter, especially at the low end, in the density function $p_V(v)$ for higher pressures.

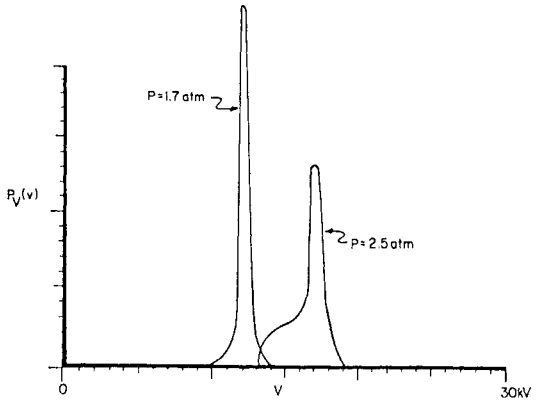

Fig. 7. Self Breakdown Voltage Probability Density Function For Different Pressures.

The pressure data was found to be of even greater importance for analyzing the different i_e cases which were studied theoretically. Figure 8 shows theoretical plots of the quantity $v'p_V(v)/(1-F_V(v))$, for the three physical cases discussed earlier: a) $i_e = i_e(m_o,v)$ m_o is a constant over the entire surface (Eq. (8)), b) $i_e = i_{eo}$ is a constant (Eq. (9)) and c) the most general case, $i_e = i_e(m,v)$ which assumes a distribution of surface field enhancements (Eq. (5)).

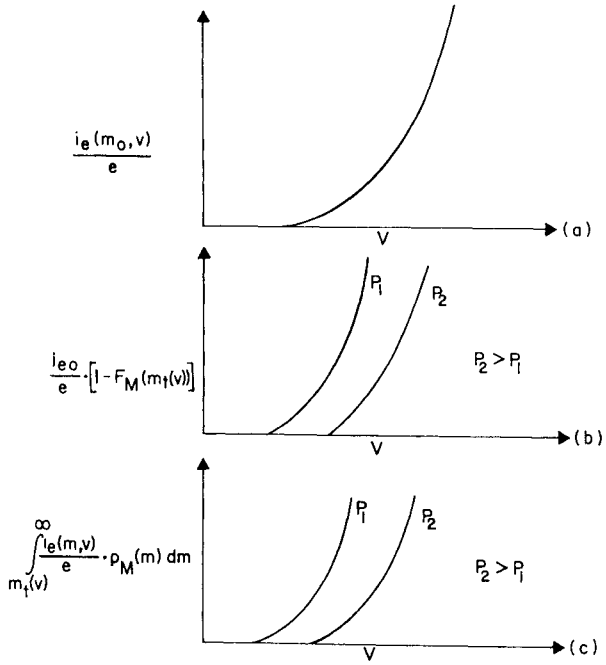

Fig. 8. Theoretical Plots of $v'p_V(v)/(1-F_V(v))$ For a) $i_e = i_e(m_o,v)$, b) $i_e = i_{eo}$ and c) $i_e = i_e(m,v)$.

Case a) illustrates that if no distribution exists in M (Eq. (10)) then an increase in pressure will correspond simply to a higher emission current because of the higher breakdown voltage, which is typical for a field dependent Schottky or Fowler-Nordheim emission mechanism [9]. However, in case b) for a fixed voltage, the increase in pressure has the effect of raising the threshold m_t required for breakdown which raises $F_M(m_t(v))$ and thus the function $v'p_V(v)/(1-F_V(v))$, is multivalued and decreases with increasing pressure (Eq. (7)). For case c) $v'p_V(v)/(1-F_V(v))$, is also multivalued and decreases with increasing pressure in the following way (Eq. (6)). For a fixed voltage and assuming the surface features do not change with pressure, the integrand is constant with increasing pressure. However, the lower limit on the integral, namely $m_t(v)$, increases with increasing pressure which has the effect of reducing the value of the function.

Figure 9 is a plot of the function $v'p_V(v)/(1-F_V(v))$, from experimental data for the pressure data of Figure 7. From this plot it is clearly seen that the experimental data are inconsistent with the theoretical results for case a) (a constant m surface). Thus, the effect of a distribution in field enhancements must be considered in the analysis of the breakdown statistics.

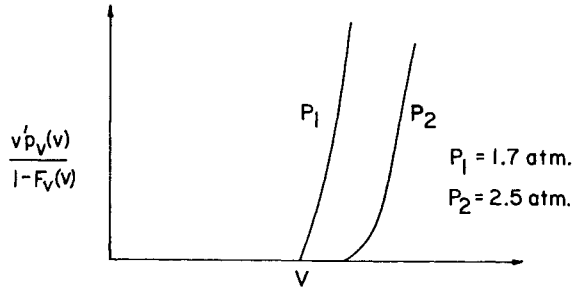

Fig. 9. Experimental Plots of $v'p_V(v)/(1-F_V(v))$.

Conclusion

Theoretical and experimental results show:

1) The spread in self-breakdown voltages in a spark gap is a function of the charging rate (v') and the cathode surface properties which determine the electron emission current i_e and the distribution of field enhancement sites $F_M(m)$.

2) Changing i_e provides a practical method for reducing the width of the self-breakdown voltage density function. This can be accomplished with an external UV source or perhaps with an electron emission agent introduced into the cathode material [18].

3) At sufficiently high pressures the cathode microstructure has adverse effects on the voltage density function.

4) The function $v'p_V(v)/(1-F_V(v))$, which can be computed directly from self-breakdown voltage data, is useful for determining the nature of i_e for a given set of conditions.

Some questions of interest which remain to be answered include:

1) Under what conditions does the cathode microstructure significantly affect the voltage stability of a spark gap?

2) What is the physical mechanism which produces the electron emission current and can it be artificially stimulated?

3) What is the mechanism(s) which produces prefires and can it be controlled?

Acknowledgments

The authors are indebted to B. Conover, P. Krothapalli, K. Rathbun and A. Shaukat for their work on the construction of the experiment and the implementation of the data acquisition system. In addition a special thanks goes to J. Clare, R. Davis, L. Heck and M. Katsaras for their work on the manuscript.

References

1) R. A. White, Proc. of 3rd IEEE International Pulsed Power Conf., Albuquerque, N.M., 360 (June 1981).

2) L. B. Gordon, et.al., IEEE Trans. on Plasma Science, PS-10, 286 (1982).

3) E. I. Zolaterev, et.al., Sov. Phys. Tech. Phys., 21, 340 (1978).

4) Physics International Report PISR-127-4 (July 1969).

5) M. T. Buttram, Sandia National Lab Report, Sand 81-1552 (1981).

6) V. A. Avrutskii, et.al., Sov. Phys. Tech. Phys., 43, 615 (1973).

7) V. A. Avrutskii, et.al., Sov. Phys. Tech. Phys., 43, 610 (1973).

8) R. M. Ness, Masters Thesis, Texas Tech University, (August 1983).

9) R. V. Hodges, et.al., Lockheed Missiles and Space Company Report, LMSC-0811978 (1982).

10) R. V. Hodges, et.al., Lockheed Missiles and Space Company Report, LMSC-0877208 (1983).

11) A. Pedersen, IEEE Trans. on Power Apparatus Systems, PAS-94, 1749 (1975).

12) S. Berger, IEEE Trans. on Power Apparatus Systems, PAS-95, 1073 (1976).

13) M. O. Hagler, et.al., Texas Tech University Pulsed Power Lab Notes, TTU-EEPP-83-1.

14) A. L. Donaldson, Masters Thesis, Texas Tech University, (August 1982).

15) S. Berger, IEEE Trans. on Power Apparatus Systems, PAS-96, 1179 (1977).

16) C. M. Cooke, IEEE Trans. on Power Apparatus Systems, PAS-94, 1518 (1975).

17) I. W. McAllister, ETZ-A, 99, 283 (1978).

18) V. I. Krizhanovskii, et.al., Sov. Phys. Tech. Phys., 26, 1204 (1981).